CrossMark

The probabilistic tsunami hazard assessment along Karnataka Coast from Makran Subduction Zone, west coast of India

Sowmya K · Ch. Patanjali Kumar · Katihally Siddappa Jayappa

Abstract Coastal tsunami amplitudes were calculated to identify areas susceptible to tsunami hazard at selected locations of the coast of Karnataka, west of India, due to earthquakes in the Makran Subduction Zone. This is the first time that the probabilistic tsunami hazard assessment along this study area has been attempted. A series of earthquake source scenarios with magnitudes of Mw 8.0, Mw 8.5, and a mega thrust of Mw 9.1 were modeled by using the Community Model Interface for Tsunami interface with the MOST model of Titov and Synolakis (J. Waterway, Port, Coastal and Ocean Engineering, 121(6), 308–316, 1995). As per the previous occurrences, the two least magnitudes are probable, while Mw 9.1 is a worst-case scenario as described by Heidarzadeh et al. (Ocean Engineering, 36(5), 368–376, 2009) and the same is reported by Burbidge et al. (Geoscience Australia Professional Opinion No. 2009/11) as high magnitude. These are not at all historical earthquakes or specifically from historical catalogues. The results of modeling show that all the seven coastal locations are inundated barely in our worst-case scenario with maximum water levels in the range of 100–200 cm. The first tsunami wave strikes the coast within 4–5 h of earthquake occurrence.

Introduction

India has two major tsunamigenic sources—Makran Subduction Zone (MSZ) and Sumatra Subduction Zone (SSZ). MSZ located in the southwestern part of Pakistan and southeastern part of Iran with a length of ~ 1000 km is one of the most tsunamigenic sources in the Indian Ocean (Hussain et al. 2002; Heidarzadeh et al. 2007, 2008a; Patel et al. 2013; Heidarzadeh and Satake 2014; Aslam et al. 2017; Zuhair and Alam 2017). Hussain et al. (2002) indicated the significant seismic risk along the Indian coast from MSZ in their probabilistic seismic risk studies. According to Heidarzadeh et al. (2008), Makran is a gradually subducting zone and is a unique area in the world as it has geological and seismological characteristics such as high sediment input of 7 km, shallow angle dip, and rate of subduction. The MSZ occurs in two segments—the west and the east, separated by a sinistral fault known as the Sonne Fault (Mokthari et al. 2008; Rajendran et al. 2008; Aslam et al. 2017; Zuhair and Alam 2017). Makran is one of the lowest-studied regions

S. K (✉) · K. S. Jayappa (✉)
Department of Marine Geology, Mangalore University, Mangalore, Karnataka 574 199, India
e-mail: sowmyakcherpulasseri@gmail.com
e-mail: ksjayappa20@gmail.com

C. P. Kumar
Indian National Centre for Ocean Information Services, Hyderabad, India
e-mail: patanjali@incois.gov.in

in the world pertaining to tsunami hazard assessment (Heidarzadeh and Kijko 2011).

The historical records of regional tsunamigenic earthquakes helped to identify the probable tsunami sources. There was conformation of potential tsunami hazard in the Arabian Sea provided by the large historical earthquakes along the MSZ (Heidarzadeh et al. 2008a; Mahmood et al. 2012). In the last 50 years, more than 50 earthquakes of magnitude Mw 8 and above have been reported in the area. Out of these, four were followed by tsunamis 1919, 1943, 1945, and 1956 (Hafeez 2007). The complete MSZ is not seismically active as the Sunda Arc or Himalaya, but it produced large earthquakes followed by tsunamis in the past (Rao 2007; Heidarzadeh et al. 2008a; Srinivasa et al. 2014; Patanjali et al. 2015). On November 28, 1945, an earthquake with a magnitude of Mw 8.1 was experienced and its epicenter was located at 25.1° N and 63.48° E (Byrne et al. 1992; Burbidge et al. 2009). The casualties were 4000 due to the low population density along the coast of Makran (Heidarzadeh et al. 2007; Mokhtari et al. 2008; Hoechner et al. 2015). This is assumed as distinctive earthquake as it was the largest calamitous event, with sufficient information accessible regarding seismic factors (Heiderzadeh et al. 2008). Byrne et al. (1992) have assessed the source parameters of this earthquake as moment magnitude of Mw 8.1, rupture length of 100–150 km, rupture width of about 100 km, slip on the fault surface of 6–7 m, strike angle of 246°, dip angle of 7°, slip angle of 89°, and depth of 27 ± 3 km. They opined that identical events could return at least every 175 years in eastern Makran, whereas Page (1979) estimates the reappearance of a similar type of earthquake along MSZ in ~ 125–250 years.

Probabilistic tsunami hazard assessment

The possibility of tsunami from MSZ is assumed by Jaiswal et al. (2008) based on the assessment of repetition of large earthquakes from history, convergence rates, and paleo-seismological results. Heidarzadeh and Kijko (2011) are pioneers for the probabilistic tsunami hazard assessment for the MSZ. Dababneh et al. (2012) studied the probable maximum tsunami due to an earthquake in the MSZ by using the Delft3D numerical model. Hoechner et al. (2015) studied the probabilistic tsunami hazard assessment for the Makran region with a

focus on maximum magnitude assumption and showed that the tsunami hazard for Makran is generally lower than for other, seismically more active subduction zones, especially concerning short-term hazards. Ambraseys and Melville (1982), Beer and Stagg (1946), and Pendse (1948) stated that large waves continued for some hours after primary waves along the Makran coast and at Karachi and Seychelles, and only one high wave at Mumbai. Neetu et al. (2011) analyzed the persistence of high waves recorded in Karachi and showed that it is due to excitation of trapped modes by the tsunami on the continental shelf. Historic seismic records indicate that most of the earthquake locations through the last 30 years are inactive. But an earthquake on 27 November 2005 with Mw 6.1 happened in the Persian Gulf region, indicating that most of the region is active for earthquakes of Mw 6–6.5 (Jaiswal et al. 2009).

Seng and Guillande (2008) modeled the worst-case scenario with magnitude of Mw 8.8 and slip of 8.89 m, intermediate-case scenario with magnitude of Mw 8.3 and a slip of 1.58 m, and best-case scenario with a magnitude of Mw 7.5 and slip of 0.79 m. The intermediate scenario simulates closely with the earthquake of 1945 of 8.3 which generated a tsunami of significant event and killed ~ 4000 people. Heidarzadeh et al. (2007 and 2008) studied tsunami hazards in the northwestern Indian Ocean by using the method of Mansinha and Smylie (1971) for initial deformation and the numerical model TUNAMI-N2 (Imamura 2006) for propagation and coastal amplification. They are concluded on the basis of the results of seismic hazard analysis that the maximum regional earthquake magnitude in the MSZ is Mw 8.3 with a repeat time of about 1000 years. Srivastava et al. (2011) have analyzed the tsunami arrival time at different locations along the west coast of India by using the following fault parameters: fault length 377 km, width 190 km, focal depth 25 km, angle between N and fault axis 265°, dip angle 7°, slip angle 90°, displacement 11 km, and earthquake magnitude 9.0 Mw (epicenter 25° 09′ N, 63° 28′ 48″ E). Srivastava et al. (2011) who considered main cities in the western coast of India have observed that the wave has reached Udupi (nearby Malpe, 209 min) earlier than Bhatkal (213 min). They attribute this to the narrower and steeper shelf, where the wave amplitude from Makran tsunami is the same as that from Dwaraka (Gujarat) (Srivastava et al. 2011). Wijesundara (2014) studied the Tsunami Risk Assessment in Weligama, Sri Lanka, based on GIS by using the ComMIT (Community

Model Interface for Tsunami) numerical model for simulated tsunami of 9.1 Mw at SSZ. Rafi and Mahmood (2010) modeled the tsunami propagation within the Gwadar coast by using the ComMIT numerical model.

Burbidge et al. (2009) have segmented the MSZ into two—H and I—as per the low hazard assessment (Mw 8.2) and high hazard assessment (Mw 9.1). And they have reported that the historical tsunami earthquake magnitude is 8.2. We estimate tsunami hazard for the coast of Karnataka by modeling three scenarios of earthquake magnitudes Mw 8.0, Mw 8.5, and Mw 9.1 by using ComMIT with the MOST (Method of Splitting Tsunami) model. The listed earthquakes used in this study are not at all historical earthquakes or historical catalogues and the lowest earthquakes are simulated closely to the 1945 tsunami. The selection of these earthquakes is based on the reference of Burbidge et al. (2009). The present study has been carried out with an aim of probabilistic tsunami hazard assessment for the Karnataka Coast which is not done so far. The inundation model, ComMIT, based on the NOAA MOST model is used for the first time for the Indian west coast with given/associated bathymetry data sets of the NOAA ComMIT server. Tsunami propagation is sensitive to sea bathymetry, and tsunami impact on the coast and flooding is sensitive to coastal topography.

Objective

The present study was carried out with an objective of probabilistic tsunami hazard assessment at seven selected locations—Ullal, Panambur, Malpe, Maravanthe, Murudeshwar, Om Beach, and Karwar—along the Karnataka coast (Table 1). This study will reveal the primary idea about how tsunami waves affect the coast in the three different tsunami scenarios and how much time the tsunami waves will take to reach the coast.

Methodology

Study area

The study area covers the Karnataka coast from 12° 45′ 27.10″ N and 74° 51′ 52.85″ E to 13° 21′ 22.36″ N and 74° 41′ 53.36″ E, a length of 320 km coastal line (Fig. 1). We used a three-level nested bathymetric grid system in this study (i.e., grids A, B, and C) as shown in Fig. 2. This coast is segmented into five C grids—C1, C2, C3, C4, and C5—which covered seven reference points (Fig. 2).

Numerical model

The MOST model (Titov and Synolakis 1995), along with the ComMIT interface for tsunami generation, wave propagation to the impact zone, and inundation along the study area, has been used in this study (Heidarzadeh and Satake 2014; Rafi and Mahmood 2010). In ComMIT-interpolated digital elevation data of ETOPO1 (2016) (one arc minute) and Shuttle Radar Topography Mission (SRTM 2016) ~90 m, data are used as the base data. This study has been conducted by considering earthquake of magnitudes 8.0, 8.5, and 9.1. The other parameters of the earthquake are taken as per the historical earthquake scenarios. The Makran Subduction Zone has been treated as the fault line prone to earthquake-activated tsunamis. In this study, wave height and wave approaching time of the tsunami at the selected locations are also considered at different magnitudes.

Model setup

Figure 3 shows the unit sources of MSZ, with each unit source having 100 km length and 50 km width. The grid extents of each C grid, the CFL condition (Courant, Friedrichs, and Lewy (CFL) stability condition), and

Table 1 The latitude and longitude extensions, CFL condition, and depth of C grids

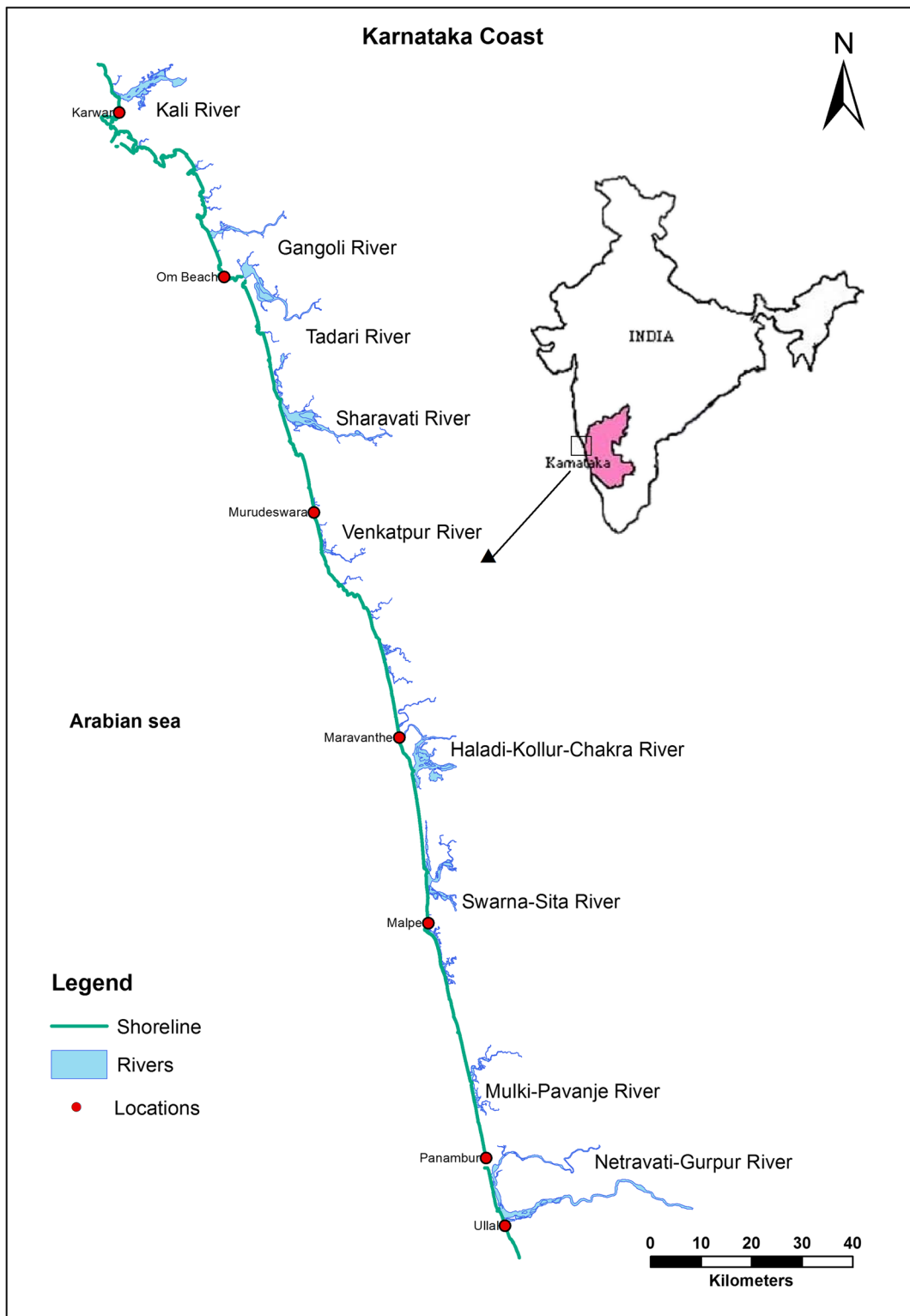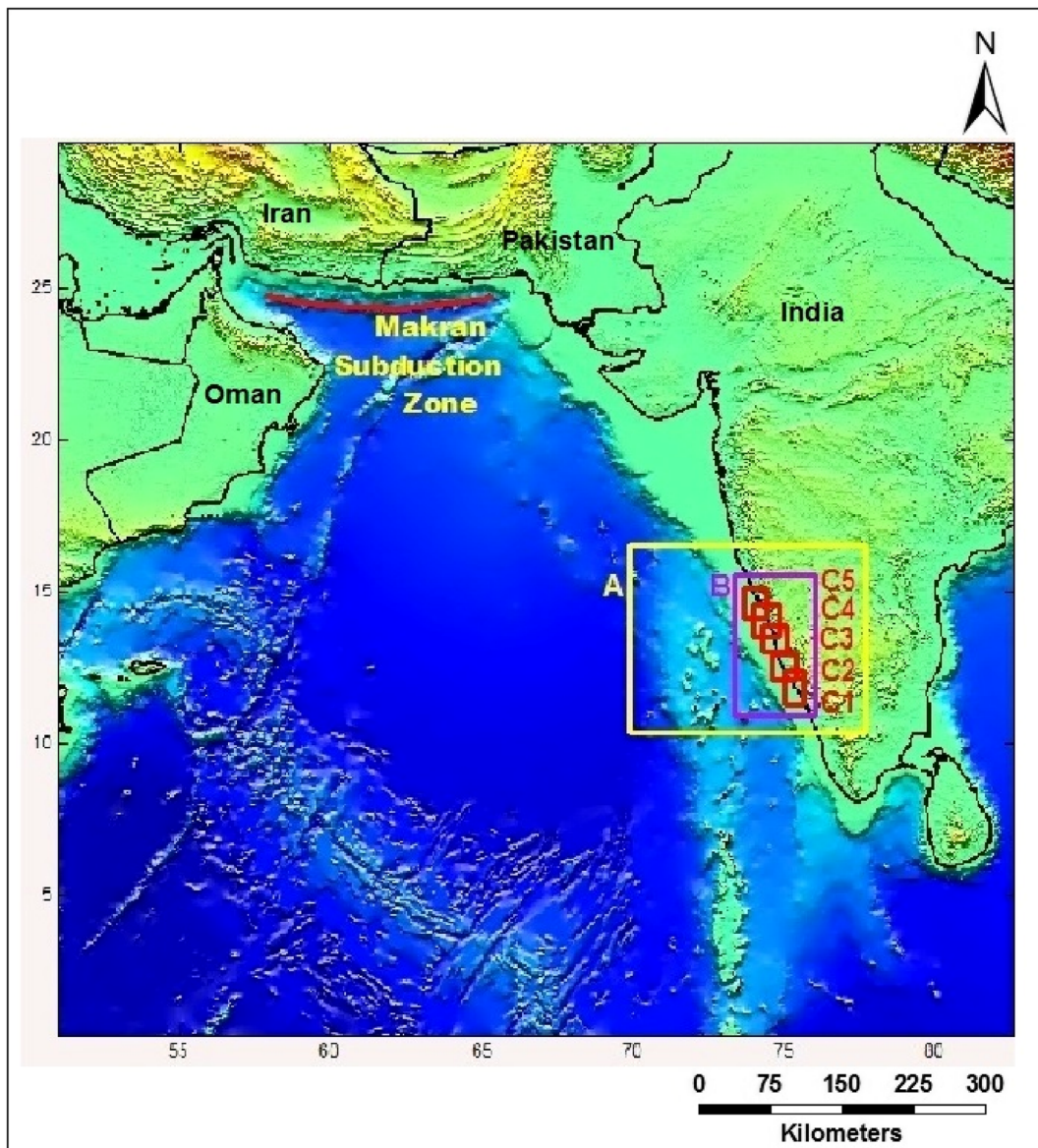| Sl. no.	C grids	Latitude extent (° north)	Longitude extent (° east)	CFL condition (s)	Max. depth of each C grid (m)
1	C1	12.6169–13.1611	74.7321–74.9321	4.73	− 37.4
2	C2	13.1279–13.7604	74.5870–74.7612	6.79	− 18.1
3	C3	13.6552–14.1485	74.4379–74.6612	5.02	− 33.0
4	C4	14.1310–14.6452	74.2630–74.4788	2.54	− 127.4
5	C5	14.5785–14.8918	74.0315–74.3190	4.22	− 46.2

Fig. 1 Location map

Fig. 2 Makran Subduction Zone and (A) grid of the study area, extending from lat. 10.00° to 16.00° north and long. 71.00° to 77.00° east, (B) grid extending from lat. 12.50° to 15.00° and long. 73.50° to 75.00°, and (C) grids of the study area

the depth of each C grid are given in Table 1. The global empirical relations in the subduction zone have been used by Papazachos et al. (2004) to determine the fault parameters of each tsunami scenario. For a tsunami scenario of Mw 8.0, the fault length is 200 km, the width is 100 km, and the slip is 2.5 m. For a tsunami scenario of Mw 8.5, the fault length is 300 km, the width is 200 km, and the slip is 5 m, while for Mw 9.1, the fault length is 600 km, the width is 200 km, and the slip is 15 m (Table 2). Table 3 explains the model parameters of each C grid.

The tsunami numerical modeling includes three stages: generation, propagation, and inundation. The generation stage of tsunami progression combines development of primary disturbance of the ocean surface due to earthquake-triggered deformation of the seafloor. The algorithm of Okada (1985) is employed to estimate the seafloor deformation based on input seismic parameters. The MOST model is applied for propagation and inundation by using the non-linear shallow-water wave equations in spherical coordinates, with Coriolis terms (Titov and Synolakis 1995), and these equations are solved
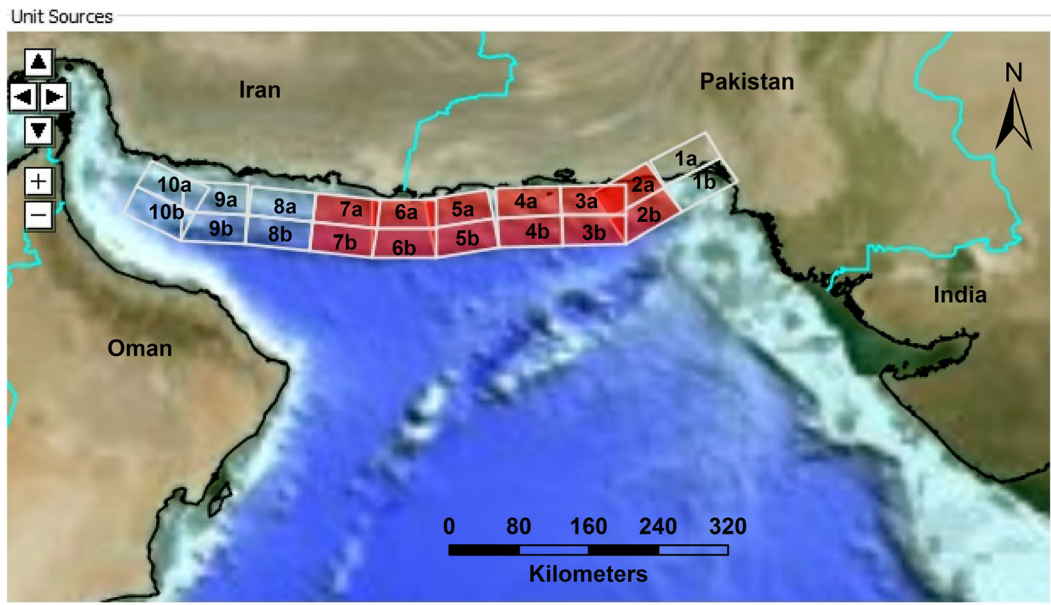
Fig. 3 Unit sources of the Makran Subduction Zone; red color blocks indicate the selection of unit sources for model simulation, and others are the remaining unit sources

numerically using a splitting method of Titov (1997). The global empirical relations in the subduction zones by Papazachos et al. (2004) are used to determine the fault size parameters such as length, width, and slip amount which relates logarithmically the fault dimensions (length, width, area, and displacement) to earthquake magnitude. The fault length (L), area (A), width (W), and displacement (D) are assumed to be represented in

terms of empirical formulae as function of magnitude (M) as described below:

Fault length (km) : $\log L$

$= 0.55\, M - 2.19$; standard deviation (SD)

$= 0.18; 6.7 < M < 9.3$ \hfill (1)

Table 2 Percentage magnitude and slip of unit sources

Sl. no.	Unit sources	% Magnitude of each unit sources			Slip		
		Mw 8.0	Mw 8.5	Mw 9.1	Mw 8.0	Mw 8.5	Mw 9.1
1	2a	0	0	8.3	0	0	15
2	2b	0	0	8.3	0	0	15
3	3a	25.0	16.7	8.3	2.5	5	15
4	3b	25.0	16.7	8.3	2.5	5	15
5	4a	25.0	16.7	8.3	2.5	5	15
6	4b	25.0	16.7	8.3	2.5	5	15
7	5a	0	16.7	8.3	0	5	15
8	5b	0	16.7	8.3	0	5	15
9	6a	0	0	8.3	0	0	15
10	6b	0	0	8.3	0	0	15
11	7a	0	0	8.3	0	0	15
12	7b	0	0	8.3	0	0	15

Table 3 Model parameters of each C grid

Sl. no.	Model parameters	C grids				
		C1	C2	C3	C4	C5
1	Minimum amplitude of input offshore wave (m)	0.0050	0.0050	0.0050	0.0050	0.0050
2	Minimum depth of offshore (m)	5.0	5.0	5.0	5.0	5.0
3	Dry land depth of inundation (m)	0.1	0.1	0.1	0.1	0.1
4	Friction coefficient	0.0009	0.0009	0.0009	0.0009	0.0009
5	Max amplitude before blow-up (m)	300.0	300.0	300.0	300	300.0
6	Time step (s)	4.5300	6.1000	4.8000	2.4300	4.0400
7	Total number of time steps in run	3200	2400	3000	5900	3600
8	Save output every n-th grid point	1	1	1	1	1

Fault area (sq.km.) : $\log A = 0.86\,\text{M}-2.82$; SD

$$= 0.25; 6.7 < \text{M} < 9.3 \qquad (2)$$

Fault width (cm) : $\log W = 0.31\,\text{M}-0.63$; 6.7

$$< \text{M} < 9.3 \qquad (3)$$

Displacement (cm) : $\log D = 0.64\,\text{M}-2.78 \qquad (4)$

As Fig. 4 shows, simulation in ComMIT starts with a new section by selecting grids A, B, and C as per the area of interest (Fig. 2). After selecting the area of interest, the unit sources (length and width of the fault) and magnitude were selected from the model interface (Fig. 3). The model runs with the input data to assess the tsunami hazard and provide time series, energy direction, and inundation as a result. From these results, the wave height at the reference point is found out.

Result

Time histories

The time history graphs are shown below in Fig. 5, for all the seven locations selected along the Karnataka Coast. The origin of time axis is defined as the origin time of dislocation. Wave height (in cm) relative to the mean sea level at a reference point and time (in h) are plotted in vertical and horizontal axes, respectively. In each case, the start of tsunami indicates the uplift of the shore. The first tsunami creates waves with a magnitude

of 9.1 reaching the coast within 4–5 h. The case scenario of Mw 9.1 produced a maximum wave height of 108 cm at Ullal, 95 cm at Panambur, and 96 cm at Malpe, and these locations were reached 4.22 h, 4.25 h, and 4.49 h,
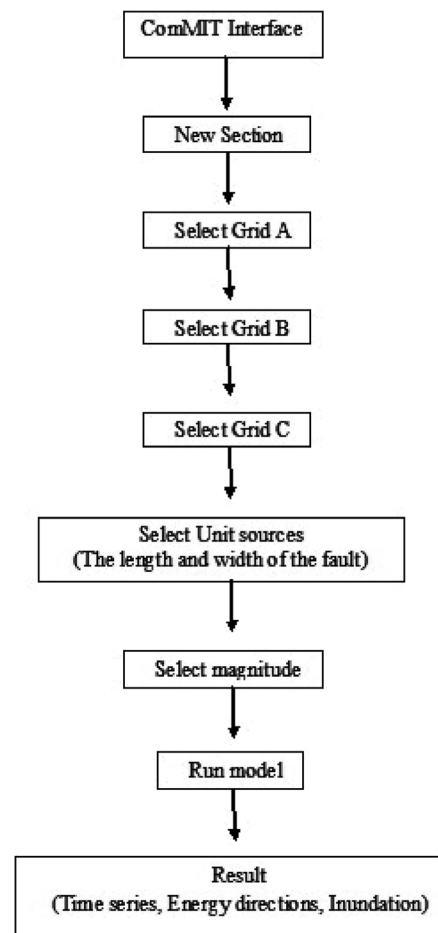
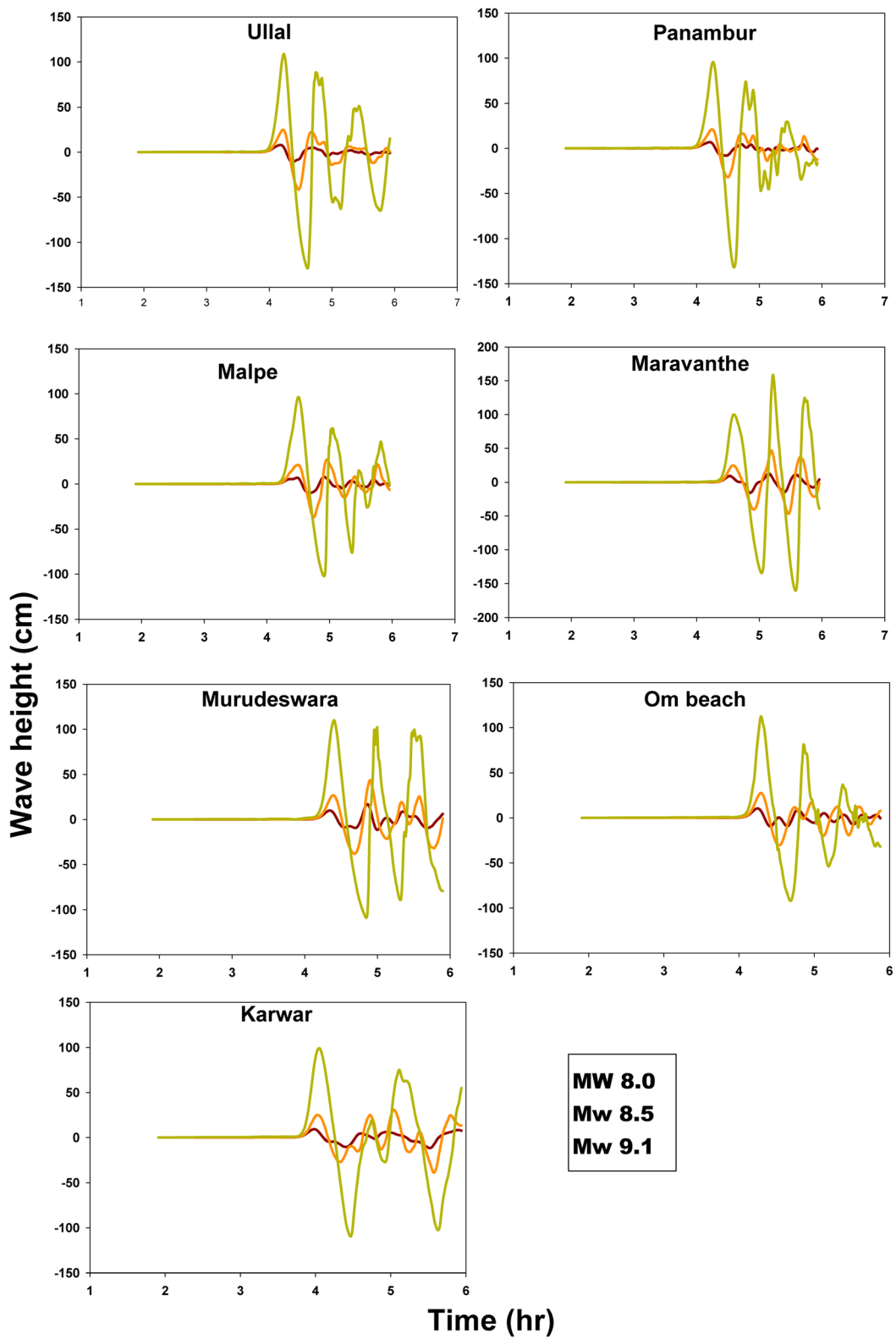**Fig. 4** Flowchart of the ComMIT model simulation

Fig. 5 Wave heights of three scenarios (Mw 8.0, Mw 8.5, and Mw 9.1) at seven locations

respectively, after the earthquake. At Maravanthe and Murudeshwar, the highest wave height and arrival time of this scenario are 158 cm at 5.21 h and 110 cm at 5.52 h, respectively. The highest computed wave height at Om Beach and Karwar also is close to 1 m, that is, 112 cm at 4.21 h and 99 cm at 4.04 h after the earthquake, respectively (Table 4).

Case scenarios

Simulation results are summarized in Table 4, and the most destructive tsunamis of the coast with a magnitude of Mw 9.1 are plotted in Fig. 6a–e. The first tsunami wave approaches the coast within 4–5 h after the origin time of dislocation. The land of the Karnataka coastal strip is slightly inundated in the Mw 9.1 scenario with a maximum water level of 100–200 cm; however, tides are not taken into account for the analysis. In the Mw 8.0 scenario, the maximum wave height on the coast is 12 cm at Maravanthe and the minimum is 6 cm at Panambur and Murudeshwar, whereas the computed maximum wave height of the Mw 8.5 scenario is 46 cm at Maravanthe and the minimum is 21 cm at Panambur and none of these areas are inundated for these scenarios. In the Mw 9.1 scenario, the maximum wave height is 158 cm at Maravanthe with slight inundation and the minimum wave height is 95 cm at Panambur.

Discussion

In this study, the maximum height of the probable tsunami wave on selected locations along the coast of Karnataka has been evaluated. It can be assumed from the simulation results that the Makran Subduction Zone can produce a tsunami, capable of causing calamitous damage to life and infrastructures on the coast. The intertidal habitat of the coast of Karnataka has rich biodiversity with a wide range of ecosystems such as sandy beaches, rocky foreshore, sea grass beds, salt marshes, and mangroves (Sowmya and Jayappa 2016). The computations made by the MOST model revealed that the wave height may reach up to 200 cm at some locations.

In most of the locations, the first and second scenarios (Mw 8.0 and 8.5) generate small tsunamis and hence do not pose threats to the west coast of India, while the third scenario (Mw 9.1) generates wave amplitudes of 95 to 158 cm. Ullal and Panambur show wave amplitudes of 108 and 95 cm, respectively, from the third scenario (Mw 9.1) (Fig. 6a). It could not be neglected because the Netravati-Gurupura Estuary, the New Mangalore Port Trust (NMPT), and other factories and refineries are situated near Panambur Beach (Sowmya and Jayappa 2016). The Ullal coast shows high wave energy compared to the adjacent beaches (Bhat and Subrahmanya 2000), and here the households and settlements are very close to the sea. The worst-case scenario result will have a catastrophic affect on the coast. Malpe Beach is also a tourist place where the wave amplitude from the worst-case scenario is 96 cm and St. Marry's Island is rich in biodiversity and near the beach, affecting the coast (Fig. 6b). At Maravanthe, the worst-case scenario of Mw 9.1 showed the wave height up to 158 cm which reaches the shore at 5.21 h, and this is the second wave (Fig. 6c). The National Highway (NH 66 Panvel-Goa-Edapally) runs very close to this beach, and the Kollur-Chakra-Halady Estuary is also very close (Sowmya and Jayappa 2016). At Om Beach, the results show minimum inundation in the Agnashini and Gangoli estuaries (Fig. 6d). The wave height shows

Table 4 The maximum wave heights at selected locations from different case scenarios

Sl. no.	Locations	Latitude (° north)	Longitude (° east)	Wave heights (cm) from 3 scenarios			Wave (Mw 9.1) reaching time (h)
				Mw 8.0	Mw 8.5	Mw 9.1	
1	Ullal	12.8097	74.8393	8	24	108	4.2254
2	Panambur	12.9374	74.8034	6	21	95	4.2556
3	Malpe	13.3599	74.6969	7	26	96	4.4956
4	Maravanthe	13.7001	74.6420	12	46	158	5.2180
5	Murudeshwar	14.0986	74.4872	6	43	110	5.5240
6	Om Beach	14.4184	74.3896	10	27	112	4.2162
7	Karwar	14.8115	74.1245	9	30	99	4.0457
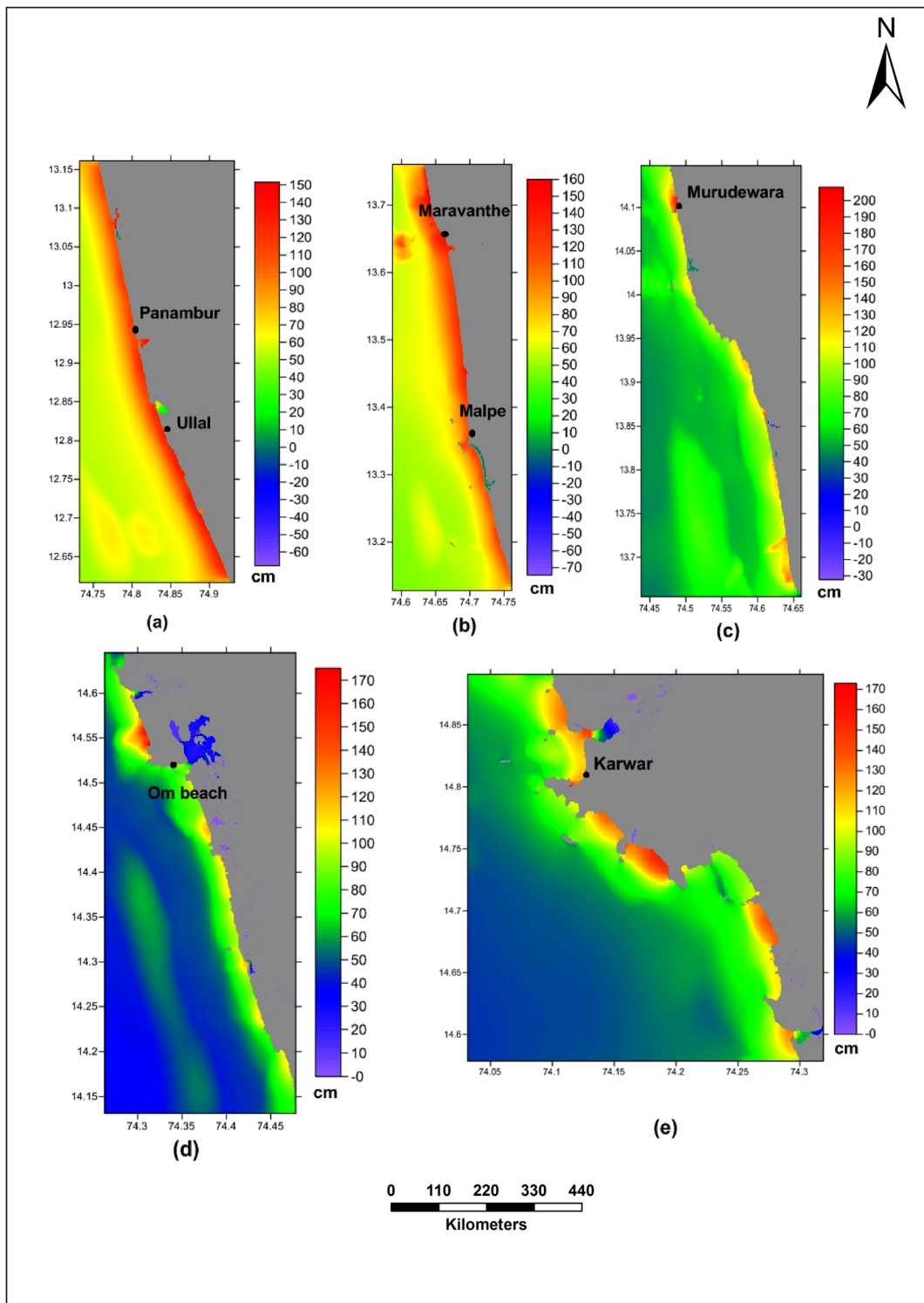
Fig. 6 Maximum wave height and inundation of each location from the case scenario Mw 9.1: **a** C grid 1, **b** C grid 2, **c** C grid 3, **d** C grid 4, and **e** C grid 5

more than 1 m at Kali River mouth (Fig. 6e), where inundation of the estuary shall be expected.

The major impact of tsunami is shown directly in the loss of human and animal life, property damage, and diseases. The Karnataka coastal population of 43.64 lakhs are directly under the threat of tsunami and infra-structures like houses (Ullal—Dakshina Kannada), fac-tories (Kodi Bengre—Dakshina Kannada), ports (New Mangalore Port—Dakshina Kannada district, Karwar Port—Uttara Kannada district, and other minor ports), naval bases (Karwar—Uttara Kannada district), ship-yards (Malpe—Udupi), roads (Maravanthe—Udupi dis-trict), and electric posts (Sowmya and Jayappa 2016), which are also vulnerable to tsunami. The environmen-tal impacts are contamination of soil and water, perma-nent changes to landscape, destruction of mangrove and coral ecosystems, solid waste and disaster debris, haz-ardous material, and toxic substances. Tsunami leads to physical changes like infrastructure damage and build-ing and bridge destruction, and chemical changes such as intrusion of saline water into the inland freshwater aquifers, eutrophication of water due to high runoff, raw sewage, and decay dead plants and animals. Flood due to tsunami is also a cause of major health problems due to contamination of water and food. The risk of infec-tious and insect-transmitted diseases is high in the peri-od of tsunami. As per the current study, Karnataka Coast is less vulnerable to tsunami. The tsunami of more than 9 Mw magnitude would affect the coast of Karnataka, and it is a worst-case scenario.

Conclusion

Tsunami hazard assessment for Karnataka Coast has not been carried out so far using ComMIT based on the NOAA MOST model, and it is the first time this model is used for the Indian west coast. In this study, three case scenarios, Mw 8.0, 8.5, and 9.1, were modeled using the MOST model with the ComMIT interface for the prob-abilistic tsunami hazard assessment along Karnataka Coast. These scenarios are selected by referring to Burbidge et al. (2009), and those are not historic earth-quakes. The first scenario shows a 6–12-cm wave height, the second scenario shows a 21–46-cm wave height, and the worst-case scenario of Mw 9.1 shows a 95–158-cm wave height along the coast of Karnataka. At Maravanthe, Murudeshwar, and Om Beaches, the maximum wave heights are noticed in the second and

third waves. The model shows that the first tsunami wave from the Makran Subduction Zone will reach the coast after 4 h of the earthquake.

Limitations

The accuracy of the result fully depended on the ba-thymetry and topography data. Because of the lack of high accuracy data, we could not estimate the inunda-tion level. The model provides unit sources as 100 km length and 50 km width, so the length width parameters were set up according to this model. The listed earth-quakes used in the study are not at all historic earth-quakes or specifically from a historic catalogue.

References

Ambraseys, N. N., & Melville, C. P. (1982). *A history of Persian earthquakes* (pp. 89–90). New York: Cambridge University Press.

Aslam, B., Muhammad, J., Muhammad, Z.I., Gulraiz, A. & Quaid, I.A. (2017) GIS mapping of tsunami susceptibility: case study of the Karachi City in Sindh, Pakistan. *Journal of Geography and Natural Disasters, 7*(1). https://doi.org/10.4172/2167-0587.1000187.

Beer, A., & Stagg, J. M. (1946). Seismic sea-wave of November 27, 1945. *Nature, 158*, 63.

Bhat, H. G., & Subrahmanya, K. R. (2000). Shoreline changes and evolution of the coastal zone in southern Karnataka, India—an analysis based on multi-temporal data. *International Archives of Photogrammetry and Remote Sensing, 33*(B7), 191–197.

Burbidge, D.R., Cummins, P.R., Mleczko, R., Latief, H., Mokhtari, M., Natawidjaja, D., Rajendran, C.P. & Thomas, C. (2009). A probabilistic tsunami hazard assessment of the Indian Ocean nations. Geoscience Australia Professional Opinion No. 2009/11.

Byrne, D. E., Syke, L. R., & Davis, D. M. (1992). Great Thrust earthquakes and aseismic slip along the plate boundary of the Makran Subduction Zone. *Journal of Geophysical Research., 97*(b1), 449–478.

Dababneh, A.J., Ferguson, B. & Barton, D.J. (2012). Probable maximum tsunami due to an earthquake in the Makran subduction zone, Presented at ISOPE.

ETOPO1 2016. http://www.ngdc.noaa.gov/mgg/global/global.html

Hafeez, H. (2007). The potential of tsunami generation along Karachi and Makran coast of Pakistan. *Pakistan Journal of Meteorology, 4*(7), 25–40.

Heidarzadeh, M. & Kijko, A. (2011). A probabilistic tsunami hazard assessment for the Makran subduction zone at the northwestern Indian Ocean, DOI https://doi.org/10.1007/s11069-010-9574-x.

Heidarzadeh, M., & Satake, K. (2014). New insights into the source of the Makran tsunami of 27 November, 1945 from tsunami waveforms and coastal deformation data. *Pure and Applied Geophysics, 172*, 621–640. https://doi.org/10.1007/s00024-014-0948-y.

Heidarzadeh, M., Pirooz, M. D., Zaker, N. H., & Mokhtari, M. (2007). Evaluating the potential for tsunami generation in southern Iran. *International Journal of Civil Engineering, 5*(4), 312–329.

Heidarzadeh, M., Pirooz, M. D., Zaker, N. H., & Synolakis, C. E. (2008). Evaluating tsunami Hazard in the Northwestern Indian Ocean. *Pure Applied Geophysics, 165*, 2045–2058.

Heidarzadeh, M., Pirooz, M. D., Zaker, N. H., Yalciner, A. C., Mokhtari, M., & Esmaeily, A. (2008a). Historical tsunami in the Makran subduction zone off the southern coasts of Iran and Pakistan and results of numerical modeling. *Ocean Engineering, 35*(8&9), 774–786.

Heidarzadeh, M., Pirooz, M. D., & Zaker, N. H. (2009). Modeling the near-field effects of the worst-case tsunami in the Makran subduction zone. *Ocean Engineering, 36*(5), 368–376.

Hoechner, A., Babeyko, A. Y., & Zamora, N. (2015). Probabilistic tsunami hazard assessment for the Makran region with focus on maximum magnitude assumption. *Natural Hazards Earth System Science, 3*, 5191–5208.

Hussain, J., Butt, K.A. & Pervaiz, K. (2002). Makran coast: a potential seismic risk belt, *Geological Bulletin*, University Peshawar, 35, 43–56.

Imamura, F. (2006). TUNAMI-N2 (Tohoku University's Numerical Analysis Model for Investigation of Near Field Tsunamis version 2) Manual draft. http://www.tsunami.civil.tohoku.ac.jp/hokusai3/J/projects/manual-ver-3.1.pdf

Jaiswal, R. K., Rastogi, B. K., & Murty, T. S. (2008). Tsunamigenic sources in the Indian Ocean. *Science of Tsunami Hazards, 27*(2), 32–53.

Jaiswal, R. K., Singh, A. P., & Rastogi, B. K. (2009). Simulation of the Arabian Sea Tsunami propagation generated due to 1945 Makran Earthquake and its effect on western parts of Gujarat (India). *Natural Hazards, 48*(2), 245–258.

Mahmood, N., Khan, K., Rafi, Z. & Finn, L. (2012). Mapping of tsunami hazard along Makran coast of Pakistan, Technical Report No. PMD-20/2012, Pakistan Meteorological Department.

Mansinha, L., & Smylie, D. E. (1971). The displacement fields of inclined faults. *Bulletin of the Seismological Society of America, 61*(5), 1433–1440.

Mokhtari, M., Abdollahie Fard, I., & Hessami, K. (2008). Structural elements of the Makran region, Oman Sea and their potential relevance to tsunamigenisis. *Natural Hazards, 47*, 185–199.

Neetu, S., Suresh, I., Shankar, R., Nagarajan, B., Sharma, R., Shenoi, S. S. C., Unnikrishnan, A. S., & Sundar, D. (2011). Trapped waves of the 27 November, 1945 Makran tsunami: observations and numerical modeling. *Natural Hazards, 59*, 1609–1618.

Okada, Y. (1985). Surface deformation due to shear and tensile faults in a half-space. *Bulletin of the Seismological Society of America, 75*, 1135–1154.

Page, W. (1979). Evidence for the recurrence of large-magnitude earthquakes along the Makran Coast of Iran and Pakistan. *Tectonophysics, 52*(1–4), 533–547.

Papazachos, B. C., Scordilis, E. M., Panagiotopoulos, D. G., Papazachos, C. B., & Karakaisis, G. F. (2004). Global relations between seismic fault parameters and moment magnitude of earthquakes. *Bulletin of the Geological Society of Greece, 36*, 1482–1489.

Patanjali, C. K., Devi, E. U., Mahendra, R. S., Sunanda, M. V., Kumar, M. P. M., Padmanabham, J., Dipankar, S., & Kumar, S. T. (2015). The admissible tsunamigenic sources region of 24 September 2013 land-based earthquake—application of backward ray tracing technique. *Current Science, 108*(9), 1712–1716.

Patel, V. M., Dholakia, M. B., & Singh, A. P. (2013). Tsunami risk 3D visualizations of Okha coast, Gujarat (India). *International journal of engineering science and Innovative Technology, 2*(2), 130–138.

Pendse, C. G. (1948). The Makran earthquake of the 28 November, 1945. *Science Notes, Indian Meteorological Department, 10*, 141–144.

Rafi, Z. & Mahmood, N. (2010). Numerical modeling of tsunami inundation for potential earthquake at Makran Subduction Zone (a case study for Gwadar Coastal Area) *Technical Report No. PMD-45/2010*.

Rajendran, C. P., Ramanamurthy, M. V., Reddy, N. T. & Rajendran, K. (2008). Hazard implications of the late arrival of the 1945 Makran tsunami. *Current Science, 95*(12), 1739–1743.

Rao, N.P. (2007). Characterization of potential tsunamigenic earthquake source zone in the Indian Ocean, Tsunami and nonlinear waves, 285–312.

Seng, D.C. & Guillande, R. (2008). Disaster risk profile of the Republic of Seychelles, United Nations Development programme.

Sowmya, K., & Jayappa, K. S. (2016). Environmental sensitivity mapping of the coast of Karnataka, west coast of India. *Ocean & Coastal Management, 121*, 70–87.

Srinivasa, T.K, Nayak, S. & Guptha, H.K. (2014). India's tsunami warning system. In A. Ismail-Zadeh, J. Urrutia Fucugauchi, A. Kijko, K. Takeuchi, & I. Zaliapin (Eds.), Extreme Natural Hazards, Disaster Risks and Societal Implications(Special Publications of the International Union of Geodesy and Geophysics, pp. 322-330). Cambridge: Cambridge University Press. https://doi.org/10.1017/CBO9781139523905.032.

Srivastava, K., Dimri, V. P., Rani, V. S., Kumar, R. K., & Narain, L. (2011). Would Makran tsunami skip India? No it would reach 8 minutes later than Ratnagiri. *Indian Journal of Geo-Marine Science, 40*(5), 620–623.

SRTM (2016). http://srtm.csi.cgiar.org/ & http://srtm.usgs.gov/

Titov, V.V. (1997). Numerical modeling of long wave runup. Ph.D. thesis, University of Southern California, Los Angeles, California, 141 p.

Titov, V. V., & Synolakis, C. E. (1995). Modeling of breaking and nonbreaking long-wave evolution and runup using VTCS-2. *J. Waterway, Port, Coastal and Ocean Engineering, 121*(6), 308–316.

Wijesundara, W. A. A. P. (2014). GIS based tsunami risk assessment in Weligma, Sri Lanka. *Universal Journal of Geoscience, 2*(8), 242–250.

Zuhair, M., & Alam, S. (2017). Tsunami impacts on nuclear power plants along Western coast of India due to a great Makran earthquake: a numerical simulation approach. *International Journal of Geosciences, 8*, 1417–1426.